Biochemistry (Moscow), Vol. 69, No. 10, 2004, pp. 1148-1157. Translated from Biokhimiya, Vol. 69, No. 10, 2004, pp. 1410-1421.

Originally published in Biochemistry (Moscow) On-Line Papers in Press, as Manuscript BM04-069, September 12, 2004.

Comparative Study of Structure and Activity of Cytotoxins from Venom of the Cobras *Naja oxiana*, *Naja kaouthia*, and *Naja haje*

A. V. Feofanov*, G. V. Sharonov, M. A. Dubinnyi, M. V. Astapova, I. A. Kudelina, P. V. Dubovskii, D. I. Rodionov, Yu. N. Utkin, and A. S. Arseniev

Shemyakin and Ovchinnikov Institute of Bioorganic Chemistry, Russian Academy of Sciences, ul. Miklukho-Maklaya 16/10, Moscow 117997, Russia: fax: (7-095) 336-1766; E-mail: alexei@nmr.ru

Received March 18, 2004
Revision received June 18, 2004

Abstract—Cytotoxins are positively charged polypeptides that constitute about 60% of all proteins in cobra venom; they have a wide spectrum of biological activities. By CD spectroscopy, cytotoxins CT1 and CT2 *Naja oxiana*, CT3 *Naja kaouthia*, and CT1 and CT2 *Naja haje* were shown to have similar secondary structure in an aqueous environment, with dominating β-sheet structure, and to vary in the twisting angle of the β-sheet and the conformation of disulfide groups. Using dodecylphosphocholine micelles and liposomes, CT1 and CT2 *Naja oxiana* were shown to incorporate into lipid structures without changes in the secondary structure of the peptides. The binding of CT1 and CT2 *Naja oxiana* with liposomes was associated with an increase in the β-sheet twisting and a sign change of the dihedral angle of one disulfide group. The cytotoxins were considerably different in cytotoxicity and cooperativity of the effect on human promyelocytic leukemia cells HL60, mouse myelomonocytic cells WEHI-3, and human erythroleukemic cells K562. The most toxic CT2 *Naja oxiana* and CT3 *Naja kaouthia* possessed low cooperativity of interaction (Hill coefficient $h = 0.6$-0.8), unlike 10-20-fold less toxic CT1 and CT2 *Naja haje* ($h = 1.2$-1.7). CT1 *Naja oxiana* has an intermediate position on the cytotoxicity scale and is characterized by $h = 0.5$-0.8. The cytotoxins under study induced necrosis of HL60 cells and failed to activate apoptosis. The differences in cytotoxicity are supposed to be related not with features of the secondary structure of the peptides, but with interactions of side chains of variable amino acid residues with lipids and/or membrane proteins.

Key words: cytotoxin, cytotoxicity, circular dichroism, secondary structure, liposomes

Snake venoms are complicated mixtures of biologically active polypeptides [1]. Cytotoxins (CT) are polypeptides found in the venom of cobras. Their polypeptide chain consists of 59-62 amino acid residues which form a spatial structure common for all CT: three β-folded loops leave the central core, which is stabilized by four disulfide bonds (Fig. 1a). The structure of CT is similar to the structure of short neurotoxins from snake venom, but the spectrum of their biological activities is quite different [1]. Some CT are cardiotoxic. At low concentrations, they increase heart rate, but at high concentrations can cause cardiac arrest [2]. The CT-induced depolarization of myocytes [3] is thought to be associated with opening of potential-dependent Ca^{2+}-channels, inhibition of K^+-channels, and also with generation of ion channels in the cell membranes by dimers or trimers of CT [4-7]. CT probably have protein targets on membranes of myocytes [3, 8-10]. Thus, cytotoxin 3 from venom of *Naja atra* can bind to proteins with molecular weights of 92, 77, and 68 kD, which are found on T-lymphocytes [11]. CT can selectively inhibit functionally important proteins such as protein kinase C and Na^+,K^+-ATPase [12-14]. The binding of CT to phospholipids is thought to determine their ability to induce lysis of various cells [1, 3, 8, 13, 15].

Numerous variations of CT in amino acid composition (Fig. 2) influence their interaction with lipid vesicles

Abbreviations: CT) cytotoxins; CT1No) cytotoxin CT1 *Naja oxiana*; CT2No) cytotoxin CT2 *Naja oxiana*; CT3Nk) cytotoxin CT3 *Naja kaouthia*; CT2Nh) cytotoxin CT2 *Naja haje*; CT1Nh) cytotoxin CT1 *Naja haje*; DOPCh) dioleoylphosphatidylcholine; DOPG) dioleoylphosphatidylglycerol; DPCh) dodecylphosphocholine; FCS) fetal calf serum; P-isomer) disulfide with a positive dihedral angle; M-isomer) disulfide with a negative dihedral angle; PBS) phosphate buffered saline; δ) angle of β-sheet twisting; ξ) dihedral angle C-S-S-C.

* To whom correspondence should be addressed.

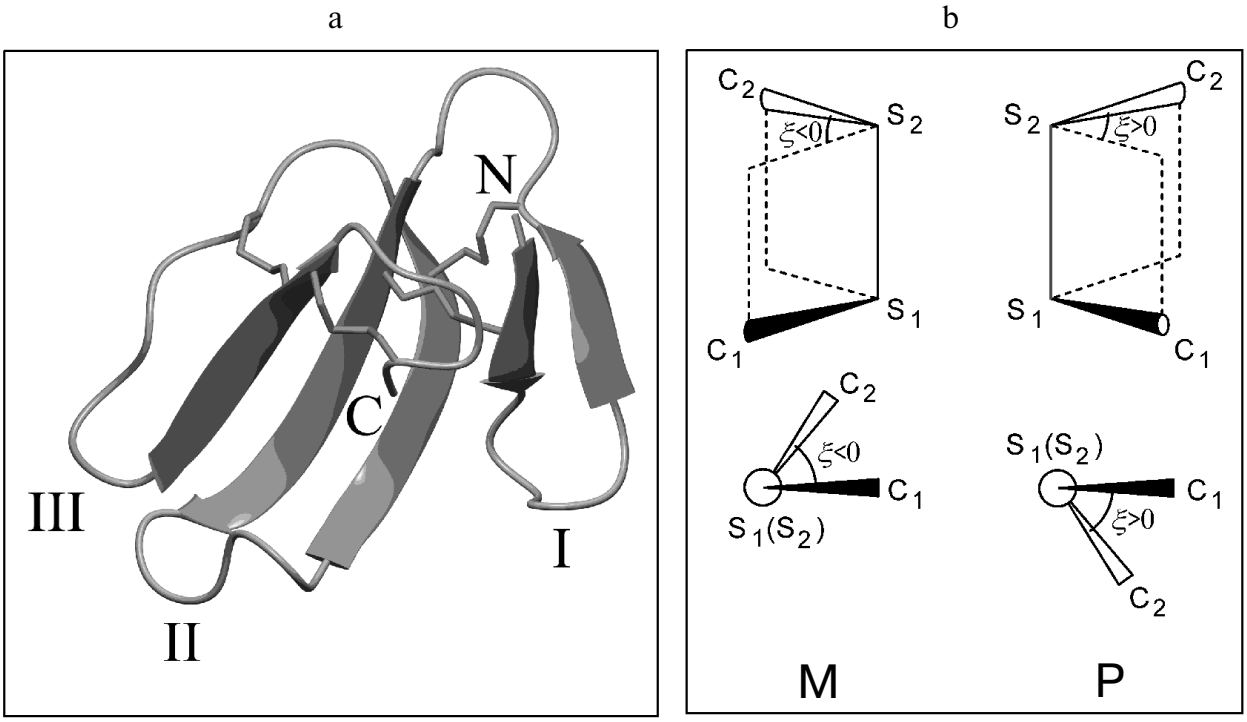

Fig. 1. a) Spatial structure and position of disulfide bonds in CT2No from NMR data [23]. The arrow-indicated wide bands show regions of the polypeptide chain, which form an antiparallel β-folded structure. The N- and C-ends are shown with letters, and roman figures indicate numbers of loops of the polypeptide chain. b) Scheme illustrating the determination of P- and M-isomers of disulfides.

```
                    10        20        30        40        50        60
CT2 N.o.    LKCKKLVPLF SKTCPAGKNL CYKMFMVAAP HVPVKRGCID VCPKSSLLVK YVCCNTDKCN
CT3 N.k.    LKCNKLIPLA YKTCPAGKNL CYKMFMVSNK TVPVKRGCID ACPKNSLLVK YVCCNTDRCN
CT1 N.o.    LKCNKLVPIA YKTCPEGKNL CYKMFMMSDL TIPVKRGCID VCPKNSLLVK YVCCNTDRCN
CT2 N.h.    LKCHKLVPPF WKTCPEGKNL CYKMYMVATP MLPVKRGCID VCPKDSALVK YMCCNTDKCN
CT1 N.h.    LKCHKLVPPV WKTCPEGKNL CYKMFMVSTS TVPVKRGCID VCPKNSALVK YVCCSTDKCN
                1-13              22-37             40-53
```

Fig. 2. Amino acid sequences of the studied CT. At the top, disulfide bonds are shown with broken lines. Solid lines at the bottom indicate three loops of CT, with numbers of amino acid residues of these loops. Variable amino acid residues are printed in bold face.

[6], ability for depolarizing myocytes [3], and hemolytic activity [6]. The CT family probably consists of several groups with different biological properties. Studies on chemically modified CT of *Naja atra* have shown that the cytotoxicity and hemolysis are determined by different functional sites [16].

Attempts to assess possible antitumor effect of snake venom have been made [17]. The main problem is that a significant antitumor effect is associated with cytotoxicity for normal cells. However, since snake venoms contain a great variety of polypeptides, they may include toxins selectively affecting malignant cells. Some fractions of venom from snakes of the *Cerastes* family were recently shown to effectively suppress tumor growth without considerable side effects [17]. But toxic effects of CT on tumor cells have been studied only in a few works [13, 18-

20], and specific features of the interaction of most CT with malignant cells remain unknown.

The present work is the first one in a series designed to study the effect of CT on tumor cells and its basic mechanisms. We think that, in addition to assessment of antitumor activity of various CT, studies on cell cultures are promising for elucidation of mechanisms of the general activity of CT. This is expected to provide a reliable basis for detection and investigation of concomitant and/or specific biological effects of CT on blood cells and myocytes. In the present work cytotoxicity was assessed of five CT from venoms of *Naja oxiana*, *Naja haje*, and *Naja kaouthia* (Fig. 2) for human promyelocytic leukemia cells HL60, mouse myelomonocytic cells WEHI-3, and human erythroleukemia cells K562. The secondary structure of CT in aqueous environment was compared by CD spectroscopy. The theory of CD effect of disulfides [21] was used to analyze CD spectra of CT, and the results were compared with NMR data on the structure of CT from *Naja oxiana* venom [22-24]: an ambiguity of the NMR data on the conformation of disulfides Cys3-Cys21 in cytotoxin CT2 *Naja oxiana* (CT2No) and Cys54-Cys59 in cytotoxin CT1 *Naja oxiana* (CT1No) was resolved, and the conformation of disulfides was characterized in CT with unknown spatial structure.

MATERIALS AND METHODS

Reagents. The following reagents were used: Tris, dioleoylphosphatidylglycerol (DOPG), dodecylphosphocholine (DPCh), and dioleoylphosphatidylcholine (DOPCh) (Sigma, USA); ethidium bromide, Trypan Blue, and HEPES (DiaM, Russia); phosphate buffered saline (PBS) (10 mM sodium phosphate buffer, 0.15 mM NaCl), L-Gln, RPMI-1640 medium, fetal calf serum (FCS), phycoerythrin-labeled annexin V (Caltag Laboratories, USA); balanced Hanks' solution (Paneko, Russia); NaCl, $CaCl_2$ "for cell cultures" (ICN, USA). Other reagents were of high grade.

CT1No and CT2No were isolated from cobra venom as described in [25], and CT1No was additionally purified by reversed-phase chromatography on a Vydac C18 column in the concentration gradient of MeCN in 0.1% CF_3COOH, with the gradient increase from 20 to 50% within 30 min. To isolate CT3 *Naja kaouthia* (CT3Nk), CT1 *Naja haje* (CT1Nh), and CT2 *Naja haje* (CT2Nh), raw venom of *Naja kaouthia* or *Naja haje* was gel filtered on a column with Sephadex G-50 superfine. The resulting major toxic fraction was separated by high performance ion-exchange chromatography on a HEMA BIO 1000CM column in an ammonium acetate gradient from 5 mM to 1 M within 1.5 h. CT were identified by MALDI mass-spectrometry and additionally purified by reversed-phase chromatography under conditions described for CT1No.

Studies on CT in solutions. CD spectra were determined in the region of 190-250 nm using a J-500 spectropolarimeter (JASCO, Japan) in a 0.1-mm cuvette at 20°C. The contribution of stray light of lipid-toxin solutions was corrected by subtracting from the spectra the baseline, which was recorded from solution of liposomes in the toxin-free buffer.

CD spectra of CT (1.4 mg/ml) in aqueous environment were recorded in 25 mM Tris-HCl buffer (pH 7.0). CD spectra of CT1No and CT2No in the presence of liposomes and micelles were obtained for solutions of the peptides (3 mg/ml) in 40 mM acetate buffer (pH 5.5) containing 1 mM EDTA. Liposomes consisting of a mixture of DOPCh and DOPG at the molar ratio of 9 : 1 were prepared by extrusion through a filter with pores 100 nm in diameter. The liposome concentration by lipids was 100 mM. Liposomes were added to the peptide solution in buffer at the lipid/protein molar ratio of 40 : 1. The DPCh/peptide molar ratio in DPCh micelles was 50 : 1. In the case of CT2No [24, 26] and CT1No (the results are in preparation for publication), these conditions ensured the complete binding of CT to liposomes and micelles.

Experiments on cell cultures. WEHI-3, K562, and HL60 cells were grown at 37°C in the presence of 5% CO_2 in RPMI-1640 medium supplemented with 2 mM L-Gln and 10% FCS. Solutions of CT (1 mM) were prepared in PBS. For experiments, the cells were planted into 12-well plates ($0.3 \cdot 10^6$ cells/ml, 3 ml RPMI-1640, 2 mM L-Gln, 10% FCS). Twenty-four hours later, aqueous solutions of CT under study were added into the wells, and the same volume of PBS was added into the control wells. To determine the cytotoxicity, the cells were incubated with CT for 3 h, washed in PBS, and stained with 0.2% Trypan Blue in PBS. The percent of stained (dead) cells was counted 10 min later. The cytotoxicity of the CT was independently determined twice on each culture. The dependence of cell death on the concentration of CT was approximated by the least square method using the Hill formula:

$$\sigma_d = 100\, C^h/(LD_{50}^h + C^h), \qquad (1)$$

where σ_d is percent of dead cells, C is concentration of CT in the medium, LD_{50} is the concentration of CT resulting in 50% death of the cells, h is an exponent. The approximation gave values of LD_{50} and h.

The type of cell death (necrosis or apoptosis) was established after incubation of the cells for 2 h with CT in the concentration, which caused the death of about 50% of the cells within 3 h. After the cells ($2 \cdot 10^6$ cells per experiment) were washed twice in balanced Hanks' solution, they were incubated for 15 min on a shaker in 200 µl of buffer (140 mM NaCl, 2.5 mM $CaCl_2$, 10 mM HEPES/NaOH, pH 7.4) supplemented with 2.5 µl of phycoerythrin-labeled annexin V from the commercial solution and ethidium bromide (10 ng/ml). After the

washing, the cells were placed under a fluorescence microscope, and the percent of living (unstained), dead (ethidium bromide in the nucleus), and apoptotic (annexin V on the plasma membrane, without ethidium bromide in the nucleus) cells was counted, as described in [27]. Such an approach allowed us to reliably determine the early stage of apoptosis even 1-2 h after the beginning of intracellular processes [27].

An Olympus BH-2 microscope (Japan) was used equipped with an epifluorescence unit and a 60× water-immersion objective (an UPLAPO60xW model, numerical aperture 1, 2), and cell images were recorded with a video camera mounted on the microscope.

RESULTS

Structure of CT by CD spectroscopy. CD spectra of CT in aqueous environment were unchanged with decrease in pH of the solution from 7.0 to 5.5 (Fig. 3), and this suggested stability of the secondary structure of CT in this range of pH. By the appearance of the CD spectra, CT are subdivided into two classes [28]: toxins with a positive band in the region of 225 nm (class II) and toxins without this band (class I). Respectively, CT1No, CT1Nh, and CT3Nk belong to class II, and CT2Nh is of class I. Despite a very weak positive signal of CT2No at 225 nm, it should be referred to class II.

A positive band with the maximum at 192 nm and a negative band with the minimum at 205-210 nm are manifestations of the dichroism of $\pi \rightarrow \pi^*$ and $n \rightarrow \pi^*$ electron transitions of amide chromophores, respectively, and indicate a significant contribution of β-folded structure to the conformation of the CT under study. A positive band in the region of 220-230 nm in the case of CT and short neurotoxins is a CD signal of disulfides [28, 29]. CD spectra of four cyto- and neurotoxins were analyzed [29], and this band could not be explained by the presence of aromatic residues (tyrosine, tryptophan), reverse turns, or non-planar peptide bonds.

In the case of CT, it was impossible to correctly calculate by CD spectra contents of canonical secondary structures, because in all programs the positive signal at 220-230 nm is described by spectra corresponding to unregulated structure, and shapes of experimental and calculated spectra do not coincide. At present, on calculating the structure it is impossible to take into account the contribution of the CD signal of disulfides. The shape typical for CD spectra of the known variety of CT is maintained, and this suggests a similarity of the secondary structure of the CT under study, both to one another and to other CT. Thus, the spatial structure of CT2No [23] may be considered as a generalized model of the structure of the CT under study (Fig. 1a). However, differences in the CD spectra (Figs. 3a and 3b) indicate some specific conformational features of CT. To describe them, we used a combined approach based on analysis of CD spectra and NMR data on the structure of CT2No [23, 24] and of CT1No (data are in preparation for publication) in water and DPCh micelles.

According to analysis of CD spectra of CT [29], the different amplitude of the signal at 190-200 nm is associated with different twisting of the β-folded sheet (hereinafter β-sheet), whereas in the region of 225 nm this difference is caused by conformation of the dihedral angle C-S-S-C (ξ) of disulfides. Note that changes in content of the unregulated structure in CT should result in the opposite sign of the change in the amplitude of signals in

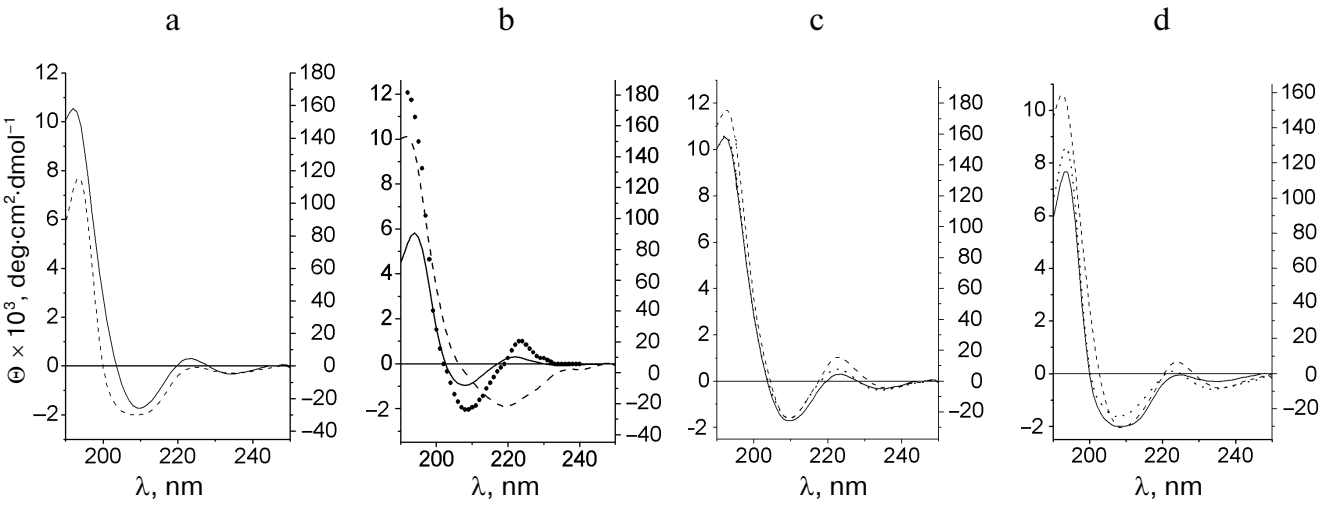

Fig. 3. CD spectra of CT. a, b) CD spectra in water (pH 7.0): a) CT1No (——) and CT2No (- - -); b) CT1Nh (——), CT2Nh (- - -), and CT3Nk (· · ·). c, d) CD spectra (pH 5.5) of CT1No (c) and CT2No (d) in water (——), in DPCh micelles (· · ·), and in liposomes (- - -). The left scale and right scales of intensity are given in molar ellipticity units per mole of peptide bonds and per mole of disulfides, respectively.

the regions of 192 and 220-225 nm, but this was not found in the analyzed spectra of CT. According to calculations [30], in weakly twisted β-sheets (angle of twisting $\delta < 5°$) amplitudes of the positive and negative signals ($\lambda \approx 195$ and 210 nm, respectively) are equal. In strongly twisted antiparallel β-sheets ($\delta > 20°$) the CD signal at $\lambda \approx 192$ nm can be 3-4-fold more intense than in the weakly twisted β-sheets [30]. Appearance of the spectra in the region of 190-210 nm (Figs. 3a and 3b) shows the strong twisting of antiparallel β-sheets. Indeed, according to NMR data for CT2No and CT1No, both the double β-sheet in the first loop (residues 1-5 and 10-14) and the triple β-sheet produced by amino acid residues of the second (residues 20-26 and 35-39) and third (residues 49-55) loops have large angles δ (Table 1, Fig. 1a). The CD signal of CT1No at $\lambda \approx 192$ nm is more intense than a similar signal of CT2No (Fig. 3a), and this agrees with a greater angle δ of the double β-sheet in CT1No (Table 1) revealed by NMR data. Similarly, the more intense signal at $\lambda \approx 192$ nm from CT2Nh and CT3Nk suggests an increased angle δ of one or both β-sheets in these CT than in CT2No, whereas CD data for CT1Nh suggest a decrease in the angle δ of its β-sheets compared to CT2No.

According to calculations [21], disulfides with the angles $\xi < 0$ (M-isomers, Fig. 1b) varying from 0 to 107° have a positive band, whereas disulfides with $\xi > 0$ (P-isomers, Fig. 1b) have a negative CD band of $\pi \rightarrow \sigma^*$ transition in the region of 220-260 nm. The intensity and position of the band depend on values of the angle ξ and valent angles C-S-S (α). At typical values of $\alpha \sim 100°$, the disulfide band has to be observed in the region of 220-230 nm at $|\xi| \approx 60°$ (the expected intensity of the band $\Theta \approx$ 12,000-17,000 deg·cm^2·dmol^{-1} disulfide). On increasing $|\xi|$ to 100°, this band has to be shifted to the region of 240-260 nm with a concomitant decrease in Θ to 6000-8000 deg·cm^2·dmol^{-1} disulfide. At $|\xi| \approx 107°$, the theory predicts a degeneration of the CD signal of disulfides [21]. According to NMR data (Table 1), only ξ values vary in CT, whereas α values change significantly less. Consequently, the position of the CD band maximum in the 220-240 nm region in CT spectra depends primarily on angles ξ of disulfides. In the region of 225-260 nm, the negative signal of amide chromophores of the β-structure is partially or completely compensated by the positive signal of amide groups of random coil structure of the polypeptide. Because it was impossible to properly take into account the contribution of these signals to the

Table 1. Values of dihedral angles C-S-S-C (ξ), valent angles C-S-S (α), and angles of β-folded sheet twisting (δ) in cytotoxins CT2No and CT1No in water and DPCh micelles by NMR data [22-24]

Disulfide	Angle, deg	CT2No in water		CT2No in micelles		CT2No in water		CT2No in micelles; variant 1
		variant 1*	variant 2	variant 1	variant 2	variant 1	variant 2	
Cys3–Cys21	ξ	−62 ± 4	104 ± 7	−62 ± 7	96 ± 10	−60 ± 3	−60 ± 4	−68 ± 3
	α_1	109 ± 2	108 ± 2	106 ± 3	103 ± 3	105 ± 1	105 ± 1	97 ± 4
	α_2	109 ± 2	108 ± 2	107 ± 3	103 ± 3	105 ± 1	105 ± 1	106 ± 2
Cys14–Cys38	ξ	−63 ± 3	−74 ± 8	−47 ± 3	−45 ± 5	−60 ± 15**	−60 ± 15**	−53 ± 4
	α_1	110 ± 1	110 ± 1	109 ± 1	109 ± 1	105 ± 1	104 ± 1	96 ± 3
	α_2	105 ± 1	105 ± 1	111 ± 2	111 ± 1	105 ± 1	105 ± 1	106 ± 3
Cys42–Cys53	ξ	87 ± 4	90 ± 3	91 ± 5	94 ± 5	80 ± 3	83 ± 2	−79 ± 3
	α_1	104 ± 3	106 ± 1	99 ± 1	101 ± 3	105 ± 1	105 ± 1	95 ± 1
	α_2	105 ± 2	106 ± 1	100 ± 1	102 ± 3	103 ± 1	103 ± 1	97 ± 3
Cys54–Cys59	ξ	84 ± 5	78 ± 5	71 ± 7	78 ± 6	−108 ± 2	70 ± 3	+62 ± 3
	α_1	103 ± 1	106 ± 2	107 ± 4	102 ± 3	104 ± 1	103 ± 1	99 ± 2
	α_2	104 ± 2	105 ± 2	102 ± 4	103 ± 2	105 ± 1	105 ± 1	96 ± 1
Double β-sheet	δ_2	40 ± 10		50 ± 11		51 ± 16		72 ± 10
Triple β-sheet	δ_3	34 ± 15		35 ± 20		35 ± 21		26 ± 23

Note: ξ is a dihedral angle C-S-S-C averaged by the set of equiprobable NMR-structures; α_1 and α_2 are averaged values of valent angles C_1-S_1-S_2 and S_1-S_2-C_2; δ_2 and δ_3 are mean angles of twisting (calculated per amino acid residue) of the double and triple antiparallel β-folded sheets, respectively (angles were calculated as described in [33]).

* Data are presented for two sets (variants 1 and 2) of equiprobable NMR structures which are different in the sign of one of the angles ξ. The CD data are consistent with variant 1. Analysis of NMR data for CT1No in micelles results in only a single variant of angles, and this variant agrees with the CD data.

** An approximate value of the angle is given based on CD data because the value of this angle cannot be determined from NMR data (see "Results").

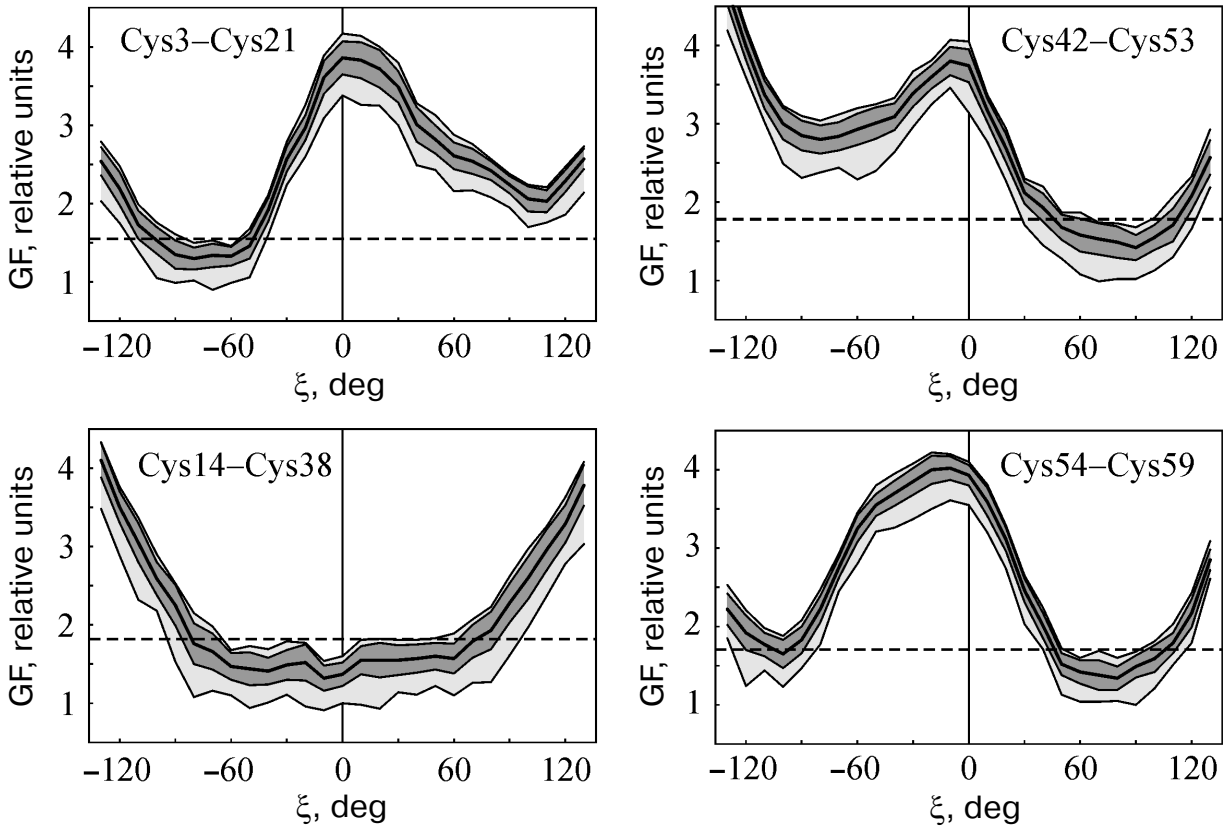

Fig. 4. Dependence of the goal function (GF) of the set of NMR structures of CT1No in water on the dihedral angle ξ of the disulfide after minimization with a CYANA program [34]. For each value of the dihedral angle, 400 random structures were minimized, and the figure presents the region of values for the 40 best structures. The most probable values of GF are shown with dark color.

resulting spectrum, our analysis was based on the hypothesis that the signal of amide chromophores in the region of 225-260 nm was approximately equal to zero.

All CT under consideration contain four conservative disulfides (Table 1), and the total signal in the CD spectrum is determined by the ratio between numbers of their M- and P-isomers. According to theory [21], the zero intensity of the CD band of CT2No disulfides in water in the region of 225 nm (Fig. 3a) suggests equal numbers of M- and P-isomers, with mutual compensation of their opposite sign signals. Conformations of three among four CT2No disulfides in water are adequately determined by NMR [23], and for Cys3-Cys21 two isomers are equiprobable (Table 1). Analysis of the CD spectrum shows that among the equiprobable (according to NMR data) isomers of Cys3-Cys21 the M-isomer is realized in water (Table 1).

In the case of CT1No in water, the signal in the region of $\pi \rightarrow \sigma^*$ transition of disulfides (Fig. 3a) is positive, thus, three or all four disulfides are likely to be M-isomers. The position of the maximum (223 nm) corresponds to the CD signal of disulfides with $|\xi| \approx 60\text{-}70^\circ$, and the value of Θ is to be equal to 12,000-17,000 deg·cm^2·dmol^{-1} [21]. The observed amplitude of the signal better corresponds to combination of three M- and one P-isomer. And the signal of the M- and P-isomer pair is mutually compensated, while two other M-isomers have $\Theta = 8800$ deg·cm^2·dmol^{-1}. It is impossible to evaluate ξ values of two disulfides with different chirality and compensated signals. But considering NMR data, these conclusions need refinement. Moreover, we shall show further that NMR studies on the CT1No structure in water fail to unambiguously determine the conformation of disulfides in the toxin, but the CD approach allows us to eliminate this uncertainty.

The non-uniqueness of NMR data is caused by poverty of NOESY-spectra of CT in cross-peaks between atoms of disulfides; moreover, constants of spin–spin interactions J (H^{α},$H^{\beta 2,3}$) and the stereospecific proton signal $H^{\beta 2,3}$ assignment prevents the establishment of a possible range of values for all five torsion angles of the side chains of cysteines. The accuracy of determination by NMR of conformation of CT1No disulfides in water was tested by the following numerical experiment: the ξ value of a disulfide was fixed in the range from –130° to 130° and the toxin structure was minimized considering all limitations. The dependence of the goal function of the CYANA program [34] on the ξ value (Fig. 4) shows

that the conformations of Cys3-Cys21 and Cys42-Cys53 are unambiguously determined from NMR data, for the conformation Cys54-Cys59 two local minimums are found (two probable conformations) with similar values of the goal function, and for Cys14-Cys38 any ξ from the range of –90° to 90° is equally admissible from the standpoint of correspondence to NMR data.

NMR spectra have been compared with CD spectra, and the conformation of Cys54-Cys59 with the angle ξ = –108° seems to be more probable of the two, whereas Cys14-Cys38 is likely to be an M-isomer with $\xi \sim -60°$ (Table 1). In this case, Cys54-Cys59 does not contribute to the spectrum because of degeneration of the CD signal at $|\xi| \sim 107°$ [21], a signal from the M- and P-isomer pair is compensated, and the resulting CD spectrum is produced by one M-isomer (Θ = 17,400 deg·cm^2·dmol^{-1}).

Based on analysis of the CD spectrum, it was suggested that in CT1Nh disulfides should be present as three M-isomers and one P-isomer. Then signals of the P- and M-isomer pair are compensated, and the band with the maximum at 222 nm is formed by two other M-isomers of disulfides ($|\xi| \approx 60\text{-}70°$, Θ = 9100 deg·cm^2·dmol^{-1}).

In the case of CT3Nk, all disulfides are supposed to be M-isomers and produce a CD signal with the maximum at 224 nm ($|\xi| \leq 70°$, Θ = 12,870 deg·cm^2·dmol^{-1}).

CT2Nh has a negative signal in the region of 220 nm (Fig. 3b) that suggests a prevalence of P-isomers of disulfides in the dipeptide structure. However, the amplitude of the signal (Θ = –28,520 deg·cm^2·dmol^{-1}) is too high even for four P-isomers of disulfides. It seems that a negative signal of the disulfides in the region of 220 nm is overlapped with a negative CD-band of the β-structure shifted to longer wavelengths (Fig. 3b). The shift of the CD signal of the β-structure suggests a change in conformational parameters of β-sheets, but the nature of these changes is unclear. By now, several CT are known which are assigned to class I by the CD spectrum [28], but no univalent correlation has been established between the negative CD signal in the region of 220 nm and specific features of the secondary structure of these polypeptides.

We have studied changes in the structure of CT1No and CT2No on binding to micelles of the detergent DPCh and with DOPCh-DOPG liposomes. The CD spectra of CT1No in water and micelles in the region of 190-210 nm (Fig. 3c) virtually coincide; consequently, the binding of CT1No with DPCh micelles does not affect the secondary structure of this cytotoxin and fails to change δ angles of its β-sheets. The absence of changes in the secondary structure is in agreement with NMR data (unpublished). However, NMR data show that parameters of the β-sheet twisting are changed: the angle δ of the double β-sheet is increased and that of the triple β-sheet is decreased (Table 1). It seems that these different changes are mutually compensated in CD spectra.

A higher than in water intensity of the positive band of CT1No in the region of 223 nm (Fig. 3c) indicates changes in the conformation of disulfides in micelles compared to aqueous solution and corresponds to three M-isomers and one P-isomer: the contribution of the M- and P-isomer pair is mutually compensated, and two other M-isomers are characterized by Θ = 13,700 deg·cm^2·dmol^{-1} and $\xi \approx -60°$. Note that by NMR data (Table 1), the conformation of CT1No disulfides in DPCh micelles is univalent, and the distribution of isomers (three M-isomers and one P-isomer) is completely consistent with the data of the CD spectra.

On incorporation of CT1No into DOPCh-DOPG liposomes, it retains a specific shape of the CD spectrum but increases intensity of the signal in the region of 192 and 223 nm (Fig. 3c). This indicates an increase in the angle δ of the β-sheet and changes in the conformation of disulfides in the absence of significant changes in the secondary structure of the polypeptide. The intensity of the positive signal at λ = 223 nm in liposomes is twice as high as in water, and this seems to indicate the transition of the disulfide Cys42-Cys53 (Table 1) from the P- into the M-conformation. As a result, in liposomes all four disulfides of CT1No are M-isomers (Θ = 15,500 deg·cm^2·dmol^{-1}, $|\xi| \approx 60\text{-}70°$). Note that according to CD data (Fig. 3c) the transition of Cys42-Cys53 between the P- and M-isomers is not associated with significant structural rearrangements in CT1No.

Comparison of the CD spectra (Fig. 3d) shows that on binding of CT2No with DPCh micelles, the β-sheet twisting is slightly increased, but the secondary structure does not change noticeably. This is confirmed by NMR data [24]: the angle δ of the double β-sheet of CT2No in micelles is greater than in water (Table 1). According to the theory of CD, the hypsochromic shift of the signal maximum from 225 to 223 nm (Fig. 3d) can be caused by a decrease in ξ value of one or several disulfides. And, in fact, by NMR data [24], the value of ξ in Cys14-Cys38 in micelles decreases to 40-50° (Table 1). Analysis of the CD spectrum shows that of two equiprobable conformations of Cys3-Cys21 predicted by NMR spectroscopy for CT2No in micelles (Table 1) M-isomer is realized, as in water.

On incorporation of CT2No in DOPCh-DOPG liposomes, the intensity of the CD signal at $\lambda \approx 192$ nm increases (Fig. 3d), which indicates an increase in the angle δ of the β-sheet. Moreover, a positive signal at λ = 223 nm appears in the spectrum of CT2No, and, based on its amplitude, the transition of one disulfide from P- to M-conformation is supposed. Thus, CT2No disulfides in liposomes are represented by three M- and one P-isomers. The contribution of the M- and P-isomer pair is mutually compensated, and two other M-isomers are characterized by Θ = 12,570 deg·cm^2·dmol^{-1} and $|\xi| \approx 60\text{-}70°$.

Effect of CT on leukemic cells. CT are significantly different in cytotoxicity for leukemic cells (Fig. 5, Table 2). Thus, equally toxic CT2No and CT3Nk were found to be 7-, 19-, 28-fold more toxic for HL60 cells than CT1No, CT2Nh, and CT1Nh, respectively, when their

concentrations resulting in the death of 50% of the cells were compared. Toxicities of CT2No and CT1No for K562 cells were approximately twofold higher than for HL60 cells. And a significant (sixfold) difference in cytotoxicities of these CT was retained. Among three cell cultures studied, mouse cells WEHI-3 were the most sensitive to CT. The relative toxicities of CT for the WEHI-3 cells were the same as described above, except the cytotoxicity of CT3Nk, which was threefold higher than the toxicity of CT2No.

Another dissimilarity of the CT under study, a cooperativity of their effects on cells, was the most distinctly detected on WEHI-3 cells. With increase in the concentration of cytotoxin, the cytotoxicity increased rather gently in the case of CT2No, CT3Nk, and CT1No and very steeply in the case of CT2Nh and CT1Nh (Fig. 5b). The assessment of Hill coefficients (h), which characterize the cooperativity of interaction between components of the system under consideration, confirmed the differences observed between the cytotoxicity dependences on CT concentration. These differences, although less pronounced, were also recorded for HL60 cells (Table 2). Note that because of different cooperativities, toxicities of CT2Nh and CT1Nh evaluated by 90% cell death are more similar to other CT as compared to toxicities evaluated by 50% cell death (Fig. 5).

CT caused necrosis of HL60 cells and did not activate apoptosis (Table 2).

DISCUSSION

Based on the known signal assignment in the CD spectrum of CT [28, 29], the present work is the first attempt to analyze the conformation of CT disulfides using the theory of the CD effect of disulfides [21]. Comparison of the results of this analysis with NMR data on the structure of CT2No and CT1No shows that the CD spectrum-based predictions about the presence of M- and P-isomers of disulfides in CT, values of their dihedral angles as well as changes in the angle values on incorporation of the peptides into micelles are in agreement with NMR data.

Analysis of the CD signal of disulfides allowed us to resolve the uncertainty in conformations of Cys3-Cys21 in CT2No and of Cys54-Cys59 in CT1No resulting from NMR data. It seems that a combined use of both methods to analyze the disulfide conformation will be necessary for determination of the detailed structures of other CT. In the present work, the conformation of disulfides in CT1Nh, CT3Nk, and partially in CT2Nh has been predicted.

Significant differences of CD spectra in the region of 190 nm are associated not with the different secondary structure of CT, but with changes in angles of the β-sheet twisting. NMR data for CT2No and CT1No in water and DPCh micelles confirm this conclusion. This fact allows

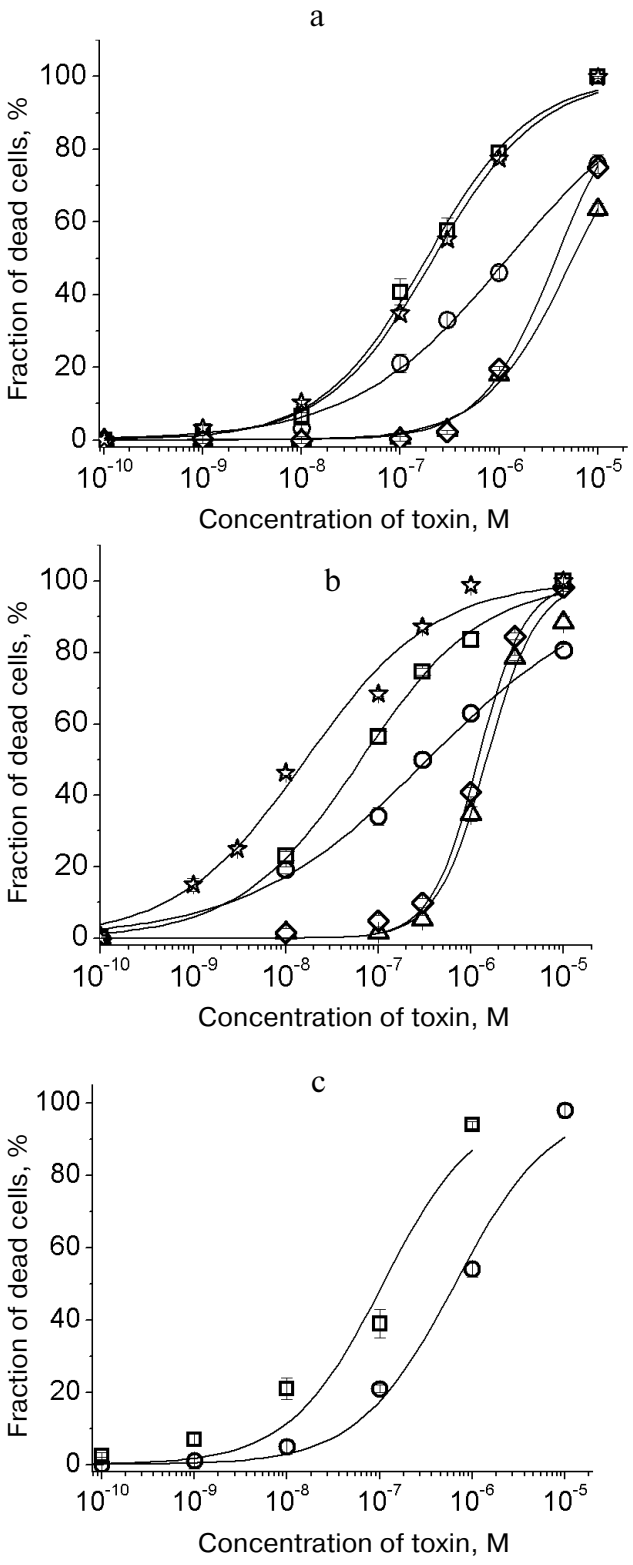

Fig. 5. Cytotoxicity of CT for HL60 (a), WEHI-3 (b), and K562 cells (c). Experimental data are presented for CT3Nk (asterisks), CT2No (squares), CT1No (circles), CT2Nh (rhombuses), and CT1Nh (triangles), as well as results of approximation of experimental dependences by the Hill model (continuous lines).

Table 2. Comparison of parameters of CT toxicity for different cells

Toxin	WEHI-3 cells		K562 cells		HL60 cells				
							cell state in culture^, %		
	LD_{50}**, nM	$h^{\#}$	LD_{50}, nM	h	LD_{50}, nM	h	living	dead	apoptotic
CT2No (P*, II[&])	65 ± 6	0.7 ± 0.1	110 ± 50	0.9 ± 0.3	180 ± 20	0.8 ± 0.1	63	35	2
CT3Nk (S, II)	16 ± 3	0.6 ± 0.1			220 ± 20	0.8 ± 0.1	66	33	1
CT1No (S, II)	340 ± 40	0.5 ± 0.1	650 ± 90	0.8 ± 0.4	1400 ± 400	0.6 ± 0.1	67	31	2
CT2Nh (P, I)	1190 ± 50	1.7 ± 0.2			3700 ± 200	1.2 ± 0.1	69	30	1
CT1Nh (S, II)	1500 ± 100	1.6 ± 0.2			5600 ± 400	1.2 ± 0.2	66	33	1
Control							93	5	2

* Subdivision of CT into P- and S-types [6].
[&] Classification of CT by CD spectra [28].
** Concentration of CT resulting in 50% death of cells for 3 h of incubation.
[#] Hill coefficient in Eq. (1).
^ Experimental conditions during studies on the mechanism of death of HL60 cells under the influence of CT are described in "Materials and Methods".

one to conclude that the structure established by NMR for CT2No and CT1No complexes with DPCh micelles is retained also on their interaction with liposomes. Changes (according to the CD data) in the conformation of a single disulfide do not change the spatial structure of CT. This finding confirms that the structures of CT2No and CT1No in DPCh micelles are adequate models that describe the interaction of these CT with liposomes and biological membranes.

In the literature two classifications of CT are proposed: by CD spectra into class II (with a positive signal in the region of 220-240 nm) and class I (no positive signal in the region of 220-240 nm); and by the presence in the polypeptides of Pro in position 30 (31) or Ser in position 28 (29) into the P- and S-type, respectively [6]. But even initially the CT classes based on CD spectra did not correlate with the activity. And in our case, cytotoxicity of CT2Nh (class I) was only slightly higher than cytotoxicity of CT1Nh (class II) but was lower than cytotoxicities of other CT of class II (Table 2). P-Type CT are different from S-type CT by the more hydrophobic second loop in the region of residues 24-34 (Fig. 2), which is thought to promote their ability for incorporation into the lipid bilayer and induction of cell lysis. The pair-wise comparison of toxicities of CT of the P- and S-types from the same source is partially consistent with this concept (Table 2): CT2No (P-type) is much more toxic for cells than CT1No (S-type); CT2Nh (P-type) is slightly more active than CT1Nh (S-type). However, the general comparison (especially on taking into account the findings on WEHI-3 cells) prevents the conclusion that P-type CT are more toxic for leukemic cells than S-type CT. Analysis of CD spectra of CT2No and CT1No shows that P- and S-type CT have no specific features of the secondary structure in both water and lipid-bound state, which would be promising for elucidation their difference in cytotoxicity. The high conservativeness of the secondary structure supports the hypothesis [31] that the difference in cytotoxicity of CT are, first of all, associated with variable amino acid residues and interaction of their side groups with lipids and/or membrane proteins.

In many cases, it is difficult to directly compare our data on cytotoxicity with the literature data because of significant differences in techniques used for measurements. The activity of CT 1, 3, and 4 from venom of *Naja atra* was assessed by inhibition of cell proliferation (on incubation with CT for 48 h), and K562 cells were shown, as in our work, to be more sensitive to CT than HL60 cells [13]. All three CT of *Naja atra* were characterized by a high cooperativity of the interaction with both K562 cells and HL60 cells. CTs from venom of *Naja atra* were two- to threefold different in cytotoxicity. Toxicity of cytotoxin 2 from venom of *Naja naja* for cells of Yoshida sarcoma [18] was similar to toxicities of CT2No and CT3Nk for HL60 and K562 cells (Table 2) and cytotoxin 2 had a high cooperativity of interaction.

It is probable that the differences of the studied CT in the cooperativity of interaction on cells (Fig. 5, Table 2) are associated with the need for producing supramolecular complexes when binding with the cell membrane to display the cytotoxic effect. Such complexing is confirmed by the following data. Crystals of cytotoxin γ from venom of *Naja nigricollis* were found to contain trimers with an internal hydrophilic channel and an external hydrophobic surface [7]. Cytotoxin A3 from venom of *Naja atra* was recently shown to form dimers on interaction with SDS molecules, and these dimers, in their turn, also could form oligomeric complexes [32]. The ability of cytotoxin A3 to induce a leakage of content of lipid vesicles was studied, and a square-law dependence of the effect on concentration of cytotoxin A3 was found; thus, this CT could form dimers on the membrane. Among the CT studied by us, CT1Nh and CT2Nh seemed to have an oligomeric type of cytotoxic effect. Other CT either had no oligomeric effect, or it was masked by highly effective cytotoxic mechanisms with $h < 2$.

With short-term incubations, the toxic effect of CT on lowly differentiated leukemic cells was manifested by permeabilization of the plasma membrane and not associated with activation of apoptosis (Table 2). This is consistent with the accepted concept of cytolysis as the general mechanism of the effect of CT on cells. Note that in highly differentiated human T-lymphocytes cytotoxin 3 of *Naja atra* increased the fraction of apoptotic cells to 15% compared to 5% in the control, on the background of death of about 50% of the cells [11].

Our data are the starting point in studies of how the structure of CT determines their interaction with cells. Based on our results, CT2No, CT1No, CT3Nk, and CT2Nh were chosen for studies, after fluorescent labeling, on mechanisms of cytotoxicity by quantitative analysis of interactions of CT with cells and of their intracellular distribution.

This work was supported by the Russian Academy of Sciences (project No. 16-12315/2003.10002-251/P-10/145-143/010403-088) and the Ministry of Industry and Science (project No. 43.106.11.0018).

REFERENCES

1. Kini, R. M. (2002) *Clin. Exp. Pharmacol. Physiol.*, **29**, 815-822.
2. Dufton, M. J., and Hider, R. C. (1988) *Pharmacol. Ther.*, **36**, 1-40.
3. Dufton, M. J., and Hider, R. C. (1991) in *Snake Toxins* (Harvey, A. L., ed.) Pergamon Press Inc., New York, pp. 259-302.
4. Wu, W., Li, Y., and Szabo, G. (1993) *FASEB J.*, **7**, A1235.
5. Rees, B., and Bilwes, A. (1993) *Chem. Res. Toxicol.*, **6**, 385-406.
6. Chien, K.-Y., Chiang, C.-M., Hseu, Y.-C., Vyas, A. A., Rule, G. S., and Wu, W.-G. (1994) *J. Biol. Chem.*, **269**, 14473-14483.
7. Bilwes, A., Rees, B., Moras, D., Menez, R., and Menez, A. (1994) *J. Mol. Biol.*, **239**, 122-136.
8. Harvey, A. L. (1991) in *Handbook of Natural Toxins* (Tu, A. T., ed.) Vol. 5, Marcel Dekker, Inc., New York, pp. 85-106.
9. Fletcher, J. E., and Jiang, M.-S. (1993) *Toxicon*, **31**, 669-695.
10. Jayaraman, G., Kumar, T. K., Tsai, C. C., Srisailam, S., Chou, S. H., Ho, C. L., and Yu, C. (2000) *Protein Sci.*, **9**, 637-646.
11. Su, S.-H., Su, S.-J., Lin, S.-R., and Chang, K.-L. (2003) *Toxicol. Appl. Pharmacol.*, **193**, 97-105.
12. Kuo, J. F., Raynor, R. L., Mazzei, G. J., Schatzman, R. C., Turner, R. S., and Kem, W. R. (1983) *FEBS Lett.*, **153**, 183-186.
13. Chiou, S. H., Raynor, R. L., Zheng, B., Chambers, T. C., and Kuo, J. F. (1993) *Biochemistry*, **32**, 2062-2067.
14. Chiou, S. H., Hung, C. C., Huang, H. C., Chen, S. T., Wang, K. T., and Yang, C. C. (1995) *Biochem. Biophys. Res. Commun.*, **206**, 22-32.
15. Harvey, A. L. (1985) *J. Toxicol. Toxin. Rev.*, **4**, 41-69.
16. Lin, S. R., Chang, L. S., and Chang, K. L. (2002) *J. Protein Chem.*, **21**, 81-86.
17. Abu-Sinna, G., Esmat, A. Y., Al-Zahaby, A. A., Soliman, N. A., and Ibrahim, T. M. (2003) *Toxicon*, **42**, 207-215.
18. Iwaguchi, T., Takechi, M., and Hayashi, K. (1985) *Biochem. Int.*, **10**, 343-349.
19. Stevens-Truss, R., Messer, W. S., and Hinman, C. L. (1996) *J. Membr. Biol.*, **150**, 113-122.
20. Hinman, C. L., Jiang, X. L., and Tang, H.-P. (1990) *Toxicol. Appl. Pharmacol.*, **104**, 290-300.
21. Kahn, P. C. (1979) *Meth. Enzymol.*, **61**, 339-378.
22. Dementieva, D. V., Utkin, Y. N., and Arseniev, A. S. (1996) *Bioorg. Khim.*, **22**, 339-352.
23. Dementieva, D. V., Bocharov, E. V., and Arseniev, A. S. (1999) *Eur. J. Biochem.*, **263**, 152-162.
24. Dubovskii, P. V., Dementieva, D. V., Bocharov, E. V., Utkin, Y. N., and Arseniev, A. S. (2001) *J. Mol. Biol.*, **305**, 137-149.
25. Grishin, E. V., Sukhikh, A. P., Adamovich, T. B., and Ovchinnikov, Yu. A. (1976) *Bioorg. Khim.*, **2**, 1018-1034.
26. Dubinnyi, M. A., Dubovskii, P. V., Utkin, Y. N., Simonova, T. N., Barsukov, L. I., and Arseniev, A. S. (2001) *Bioorg. Khim.*, **27**, 102-113.
27. Feofanov, A., Grichine, A., Karmakova, T., Pljutinskaya, A., Lebedeva, V., Filyasova, A., Yakubovskaya, R., Mironov, A., Egret-Charlier, M., and Vigny, P. (2002) *Photochem. Photobiol.*, **75**, 633-643.
28. Grognet, J. M., Menez, A., Drake, A., Hayashi, K., Morrison, I. E., and Hider, R. C. (1988) *Eur. J. Biochem.*, **172**, 383-388.
29. Hider, R. C., Drake, A. F., and Tamiya, N. (1988) *Biopolymers*, **27**, 113-122.
30. Illangasekare, M. P., and Woody, R. W. (1986) *Biophys. J.*, **49**, 296a.
31. Golovanov, A. P., Efremov, R. G., Jaravine, V. A., Vergoten, G., and Arseniev, A. S. (1995) *FEBS Lett.*, **375**, 162-166.
32. Forouhar, F., Huang, W. N., Liu, J. H., Chien, K. Y., Wu, W. G., and Hsiao, C. D. (2003) *J. Biol. Chem.*, **278**, 21980-21988.
33. Chou, K.-C., Pottle, M., Nemethy, G., Ueda, Y., and Sheraga, H. A. (1982) *J. Mol. Biol.*, **162**, 89-112.
34. Herrmann, T., Guntert, P., and Wuthrich, K. (2002) *J. Mol. Biol.*, **319**, 209-227.